Characterizing Triplet States of Quinonoidal Dinitrenes as a Function of Conjugation Length

Masaki Minato and Paul M. Lahti*

Contribution from the Department of Chemistry, University of Massachusetts, Amherst, Massachusetts 01003

Received October 18, 1996[⊗]

Abstract: Photolysis of *para,para′*-diazide precursors in 2-methyltetrahydrofuran gives biradical ESR spectra assignable to quinonoidal dinitrenes with excited triplet biradical states. The zero field splitting (zfs) parameters for the biradicals at 77 K are as follows: 1,4-phenylenedinitrene ($|D/hc| = 0.169$ cm^{-1}, $|E/hc| = 0.004$ cm^{-1}); 4,4′-biphenyldinitrene ($|D/hc| = 0.188$ cm^{-1}, $|E/hc| \leq 0.002$ cm^{-1}); 4,4′-stilbenedinitrene ($|D/hc| = 0.122$ cm^{-1}, $|E/hc| < 0.002$ cm^{-1}); 1,4-bis(*p*-nitrenophenyl)buta-1,3-diene ($|D/hc| = 0.0865$ cm^{-1}, $|E/hc| < 0.002$ cm^{-1}); 1,8-bis(*p*-nitrenophenyl)octa-1,3,5,7-tetraene ($|D/hc| = 0.0442$ cm^{-1}, $|E/hc| < 0.001$ cm^{-1}). These zfs parameters are inconsistent with simple dipole−dipole analysis of the ESR spectra in localized biradicals, but are reconcilable with a spin-polarized model involving the π-electrons of the biradicals.

Introduction

As part of our studies of interelectronic exchange interactions in open-shell molecules, we have investigated intramolecular exchange in dinitrene model systems.[1−11] By studying these and other organic diradicals and polyradicals, we aim to understand better the structure−property relationships controlling ground state spin multiplicity. Such information is a critical part of efforts to design and synthesize new, molecule-based magnetic materials that incorporate organic building blocks as part of their structures.[12−15]

bis(arylnitrene)

quinonoidal dinitrene
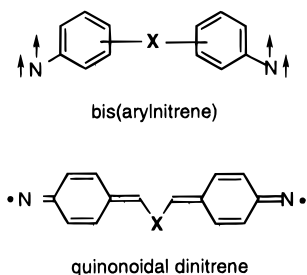
One type of system of considerable interest is the class of quinonoidal dinitrenes. These are expected to have two lo-calized, unpaired electrons in σ-type orbitals with cojugated π-clouds that allow the possibility of π-spin polarization. Through such a spin-polarized mechanism, indirect communication between the conjugatively isolated unpaired electrons is enabled. We were interested in probing how quickly such an indirect exchange interaction would decrease as a function of conjugation length in the quinonoid structure. In principle, dilution of spin delocalization would lead to isolation of the unpaired spins on the nitrogen termini of these molecules, resulting in a pair of non-interacting radicals. Since spin polarization is an important exchange mechanism, these molecules are worthy of investigation, even though they are too unstable to be of practical use. Herein we report details on generation and variable temperature ESR spectroscopy of the biradicals 1,4-phenylenedinitrene, 4,4′-biphenyldinitrene, 4,4′-stilbenedinitrene, 1,4-bis(*p*-nitrenophenyl)-1,3-butadiene, and 1,8-bis(*p*-nitrenophenyl)-1,3,5,7-octatetraene, **1−5** respectively.

Synthetic Methods. Figure 1 details the syntheses of diazide precursors **6−10**. Standard chemical transformations were used to reduce appropriate dinitroarenes to the corresponding diamines. The diamines were then transformed into diazides via diazotization/azidification by the Sandmeyer route. All diazides were thermally stable colored solids that rapidly discolored in room light. They can be stored for many months in the dark at 10 °C or less.

Computational Methods. All computations were carried out on a Silicon Graphics Indigo R4000 computer. Geometry optimizations were performed using either the GAUSSIAN94[16a] or GAMESS[16b] programs using the standard criteria within these programs for convergence. Spin density calculations on dinitrene **1** were carried out at a fixed geometry using the MELDF suite of programs developed by Davidson and co-workers.[17] Spin density plots were visualized using SPARTAN (version 4.1.1) by Wavefunction Inc.

[⊗] Abstract published in *Advance ACS Abstracts,* February 15, 1997.

(1) Lahti, P. M. In *Research Trends*; Menon, J.; Ed.; Council of Scientific Research Integration: Trivandrum, India, 1992; Vol. 3, pp 179−192.

(2) Ling, C.; Minato, M.; Lahti, P. M.; van Willigen, H. *J. Am. Chem. Soc.* **1992**, *114*, 9959.

(3) Minato, M.; Lahti, P. M. *J. Am. Chem. Soc.* **1993**, *115*, 4532.

(4) Minato, M.; Lahti, P. M. *J. Phys. Org. Chem.* **1993**, *6*, 483.

(5) Ling, C.; Lahti, P. M. *J. Am. Chem. Soc.* **1994**, *116*, 8784.

(6) Minato, M.; Lahti, P. M. *J. Phys. Org. Chem.* **1994**, *5*, 495.

(7) Ling, C.; Lahti, P. M. *Chem. Lett.* **1994**, 1357,2447.

(8) Lahti, P. M.; Minato, M.; Ling, C. *Mol. Cryst. Liq. Cryst.* **1995**, *271*, 147.

(9) Ichimura, A. S.; Sato, K.; Kinoshita, T.; Takui, T.; Itoh, K.; Lahti, P. M. *Mol. Cryst. Liq. Cryst.* **1995**, *272*, 57.

(10) Minato, M.; Lahti, P. M. *J. Phys. Org. Chem.* **1991**, *4*, 459.

(11) Ling, C.; Lahti, P. M. *Chem. Lett.* **1993**, 769−772.

(12) Miller, J. S.; Dougherty, D. A., Eds. *Mol. Cryst. Liq. Cryst.* **1989**, *176*, 1.

(13) Gatteschi, D.; Kahn, O.; Miller, J. S.; Palacio, F. *Magnetic Molecular Materials*; Kluwer Academic Publishers: Dordrecht, The Netherlands, 1991; Vol. 198E.

(14) Iwamura, H.; Miller, J. S., Eds. *Mol. Cryst. Liq. Cryst.* **1993**, *232−233*, 1.

(15) Miller, J. S.; Epstein, A. J., Eds. *Mol. Cryst. Liq. Cryst.* **1995**, *271−274*, 1.

(16) (a) Frisch, M. J.; Trucks, G. W.; Schlegel, H. B.; Gill, P. M. W.; Johnson, B. G.; Robb, M. A.; Cheeseman, J. R.; Keith, T.; Petersson, G. A.; Montgomery, J. A.; Raghavachari, K.; Al-Laham, M. A.; Zakrzewski, V. G.; Ortiz, J. V.; Foresman, J. B.; Peng, C. Y.; Ayala, P. Y.; Chen, W.; Wong, M. W.; Andres, J. L.; Replogle, E. S.; Gomperts, R.; Martin, R. L.; Fox, D. J.; Binkley, J. S.; Defrees, D. J.; Baker, J.; Stewart, J. J. P.; Head-Gordon, M.; Gonzalez, C.; Pople, J. A. Program Gaussian 94, Revision B.3; Gaussian, Inc.: Pittsburgh, PA, 1995. (b) Schmidt, M. M.; Baldridge, K. K.; Boatz, J. A.; Jensen, J. H.; Koseki, S.; Gordon, M. S.; Nguyen, K. A.; Windus, T. L.; Elbert, S. T. *QCPE Bull.* **1990**, *10*, 52 (Program GAMESS).
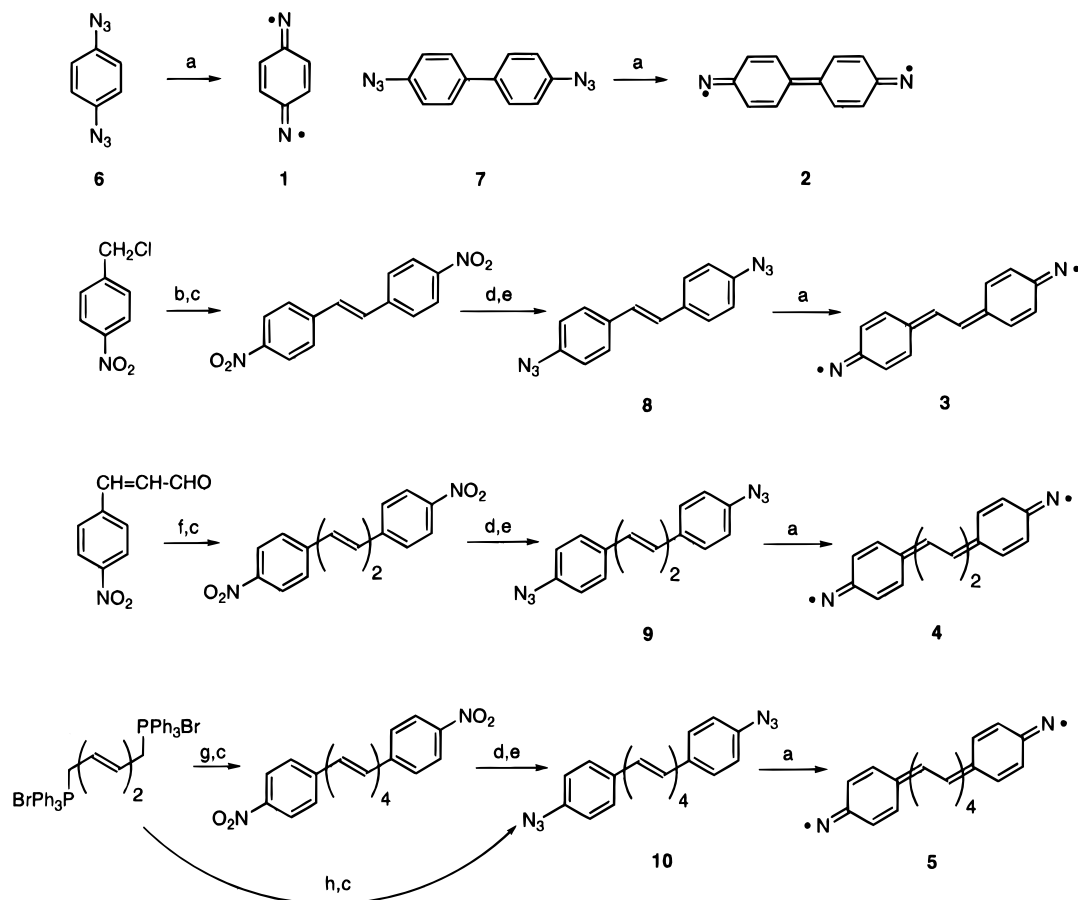
Figure 1. Synthesis of diazides **6**−**10** and generation of dinitrenes **1**−**5**: (a) MTHF, 77 K, $h\nu$ > 300 nm, 5 min; (b) NaOH/acetone/EtOH, heat; (c) I_2/hexane or acetone, heat; (d) $SnCl_2 \cdot H_2O$/EtOH, heat or (for **10**) Fe/dimethylformamide/HCl, heat; (e) $NaNO_2$, aq H^+, then NaN_3; (f) (*p*-nitrobenzyl)triphenylphosphonium bromide/EtOH/LiOEt; (g) *p*-nitrobenzaldehyde/EtOH/NaOEt; (h) *p*-azidobenzaldehyde/EtOH/NaOEt.

Results

X-band ESR spectra in the 100−9900 G range produced by 5 min each of photolysis at 77 K of **6**−**10** in 2-methyltetrahydrofuran (MTHF) are shown in Figures 2a−e. Similar spectra could be generated in ether/pentane/alcohol (EPA) glasses, but all work described below was carried out in the simpler solvent system. All spectra can be divided into three major regions: (1) radical spectral peaks in the $g = 2$ region, (2) mononitrene peaks in various positions over the 5800−6800 G region, and (3) biradical spectral features attributable to $\Delta M_s = 1$, 2 transitions. The spectral features show considerable thermal stability at 77 K, but fade rapidly and irreversibly when the matrix is warmed above 85 K. The radical features in the $g = 2$ region often dominate the spectra, and may be attributed to various species, including the photolysate of MTHF and the products of reaction by the nitrenes or dinitrenes with MTHF. We did not study the $g = 2$ spectral region, save to note that it increases with photolysis time, and is substantially decreased by photolysis at wavelengths >300 nm. As part of the process of evaluating the biradical portions of the spectra, we carried out triplet ESR spectral simulations using the eigenfield method,[18] the results of which are shown in Figure 3. The zfs values from the simulations for $|D/hc|$ and $|E/hc|$ of **1**−**5** are summarized in Table 1.

Figures 4a−e show temperature vs intensity plots for the biradical spectra of **1**−**5**. The decreasing intensity of the spectra at <30 K can make them difficult to observe, and clearly shows the spectra to be due to thermally populated excited states. Due to the instability of the biradical spectra in MTHF at >85 K, we were limited in our ability to investigate the Curie behavior of the dinitrenes. If one assumes thermal equilibrium between ground state singlet and excited state triplet states, the spectral intensity I of the ESR active triplet state is given by eq 1:[19]

$$IT = \frac{3 \exp(-2J/RT)}{1 + 3 \exp(-2J/RT)} \qquad (1)$$

J is the exchange coupling between the unpaired electrons, T is absolute temperature, and R is 1.987 cal/(mol·K). The singlet−triplet gap $\Delta E_{T-S} = 2J$ for a biradical. Nonlinear least-squares curve fitting of the data[20] in Figure 4 to eq 1 yields the J values for **1**−**5** that are listed in Table 1; the fitted curves are shown in the figure.

The spectral intensities by this model should exhibit maxima, as is observed only for **5** at temperatures below the MTHF thawing point. This limitation renders our estimates of J somewhat imprecise, despite the apparently similar shapes of the curves for **1**−**4**. Studies in solid state matrices may eventually allow a wider temperature range for these Curie studies. For example, in a *p*-dinitrobenzene matrix dinitrene **1** is stable for many months at room temperature.[9] Under these conditions, $\Delta E_{T-S} = 820$ cal/mol for **1**, reasonably similar to

(17) Davidson, E. R.; Feller, D.; Daasch, R.; Langhoff, S.; Elbert, S. T.; Martin, R.; Rawlings, D.; McMurche, L.; Cave, R.; Phillips, P.; Day, S.; Iberle, K.; Nitzsche, L.; Stenkamp, L.; Frey, G.; Jackels, C. Program MELDF, Quantum Chemistry Group, Indiana University, Bloomington, IN, 1988 (*QCPE* 580).

(18) Teki, Y.; Fujita, I.; Takui, T.; Kinoshita T.; Itoh, K. *J. Am. Chem. Soc.* **1994**, *116*, 11499. Cf. also: Sato, K. Ph.D. Thesis, Osaka City University, 1992.

(19) Bleaney, B.; Bowers, K. D. *Proc. R. Soc. London, A* **1952**, 214.

(20) All nonlinear least-squares analyses were carried out using the program PSI-Plot v. 3.0 from Polysoft Corp in Salt Lake City, UT.
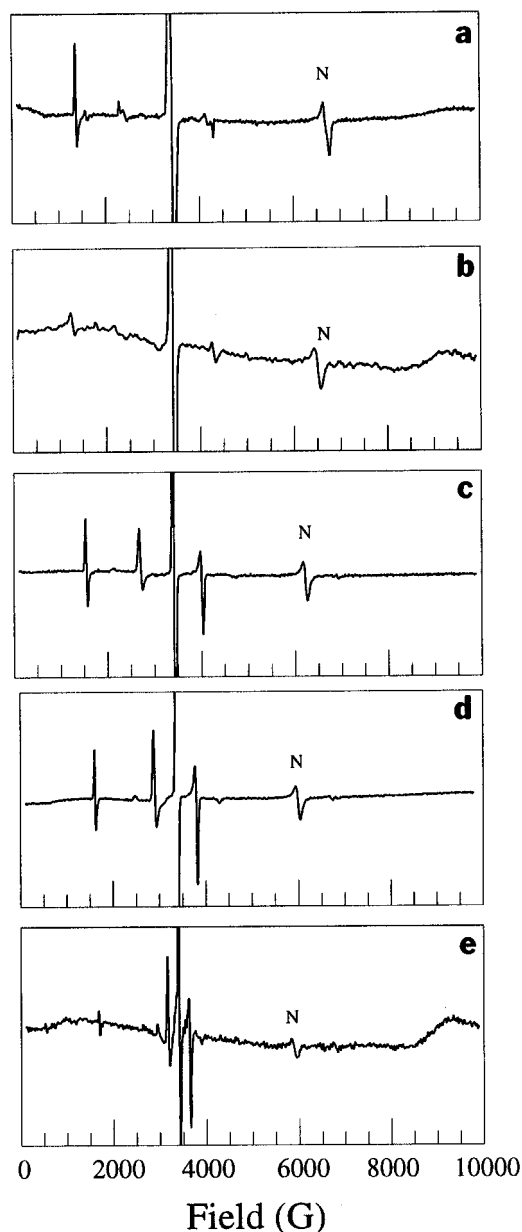
Figure 2. Full-range ESR spectra from photolyses of **6**−**10** at 77 K in MTHF (spectral traces a−e, respectively). The range in all spectra is 100−9900 G. All spectra were obtained at ν_0 = 9.5−9.6 GHz. The symbol "N" denotes a mononitrene peak.

the value of 580 cal/mol found in glassy MTHF. Although solid state studies have complications associated with possible microaggregation of photoprecursors and with guest−host interactions in the crystal lattice (leading to different average conformations in solid versus frozen solution), they hold promise for considerable future work. For the remainder of this contribution, however, we will confine ourselves to describing frozen MTHF matrix work.

The mononitrene region of the spectrum exhibits some complexity as a function of time of photolysis and of precursor. Weak mononitrene peaks may be observed with considerably larger zfs than the major peaks associated with monodeazetation, especially in the longer conjugated systems. We tentatively assign these to mononitrenes in which considerable twisting of the π-network decreases conjugation of the π-electron at the nitrene site, leading to an increased zfs. We are uncertain whether such twisting is due to a conformational mix of the diazide precursors in the frozen matrix before photolysis or whether twisting occurs during photolysis.

As an additional complication, other work has suggested that additional mononitrenes (with zfs slightly smaller than those of the monodeazetation products) may be formed by a slow dark reaction of biradicaloid dinitrenes with MTHF.[21] We found the temperature versus intensity behavior for the ESR spectra of **1**−**5** to be reproducible over the time scale of our experiments, hence this latter reaction should cause only limited imprecision in our results.

Discussion

Qualitative Zero Field Splitting Trends in 1−5. Biradical **1** was first generated in powdered matrix in trailblazing work by Trozzolo *et al.*[22] and was further analyzed in frozen solution matrix by Singh and Brinen,[23] who reported the zfs splitting as $|D/hc|$ = 0.171 cm^{-1} (no *E*-value was described, although the literature spectrum showed $|E/hc|$ > 0). Singh and Brinen also identified a dimerization mechanism for **1** under high concentration conditions. Subsequently, we reported[4] the $|D/hc|$ and $|E/hc|$ zfs parameters for **1** in frozen MTHF solution, as well as the qualitative singlet ground state nature of **1**. The present work (Table 1) found ΔE_{T-S} for **1** based on Figure 4a.

Biradical **1** has been known for a considerable time,[22] but its identification as a singlet biradical was an important theoretical test of exchange models. In a simple molecular orbital (MO) approximation, one may apply a Hund's rule type argument to predict that localized biradicals such as **1**−**5** would have triplet ground states, since all have nearly degenerate SOMOs and two unpaired electrons. But, by valence bond (VB) or spin-polarization (SP) arguments, all of **1**−**5** are expected to have singlet ground states by a small margin. The experimental finding of singlet ground states for all of **1**−**5** is a powerful argument for the VB and SP arguments that have been eloquently set forth by Itoh and co-workers in their discussions of biradical dicarbenes such as **11** and **12**,[24] which are related by connectivity to **1** and **2** and which also have singlet ground states with low-lying triplet excited states. Any perturbations by the higher electronegativity of nitrogen in **1**−**5** are insufficient to reverse the simple qualitative effects of the SP model. Moreover, biradicals **1** and **2** are structurally simpler tests of the VB and SP models than are **11** and **12**, which have conformational flexibility about their divalent carbons that is impossible for the corresponding dinitrenes.
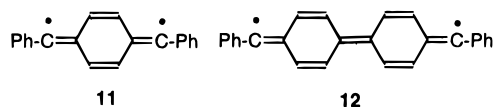
Preliminary ab initio SCF-MO-CI computations on biradical **1** showed nearly degenerate $^3B_{1u}$ and ^1A_g states, with a slight preference for the triplet in violation of the experimental result.[25] More recent post-Hartree−Fock computations reverse this preference, and find the ^1A_g state to lie below $^3B_{1u}$ by 890 cal/mol when the two states are both optimized at a 6−31G* CASSCF(8,8) level of theory,[26] in very good agreement with the experimental gap of 500−900 cal/mol. The post-Hartree-Fock optimizations are necessary to obtain the slight differences in geometry between the $^3B_{1u}$ and ^1A_g states which lead to the

(21) Harder, T.; Bendig, J.; Scholz, G.; Stösser, R. *J. Am. Chem. Soc.* **1996**, *118*, 2497.
(22) Trozzolo, A. M.; Murray, R. W.; Smolinsky, G.; Yager, W. A.; Wasserman, E. *J. Am. Chem. Soc.* **1963**, *85*, 2526.
(23) Singh, B.; Brinen, J. S. *J. Am. Chem. Soc.* **1971**, *93*, 540.
(24) Itoh, K. In *Magnetic Molecular Materials, NATO ASI Series*; Gatteschi; D., Kahn, O., Miller, J. S., Palacio, F., Eds.; Kluwer: Dordrecht, The Netherlands, 1991; p 67.
(25) Ichimura, A. S.; Lahti, P. M. *Mol. Cryst. Liq. Cryst.* **1993**, *233*, 33.
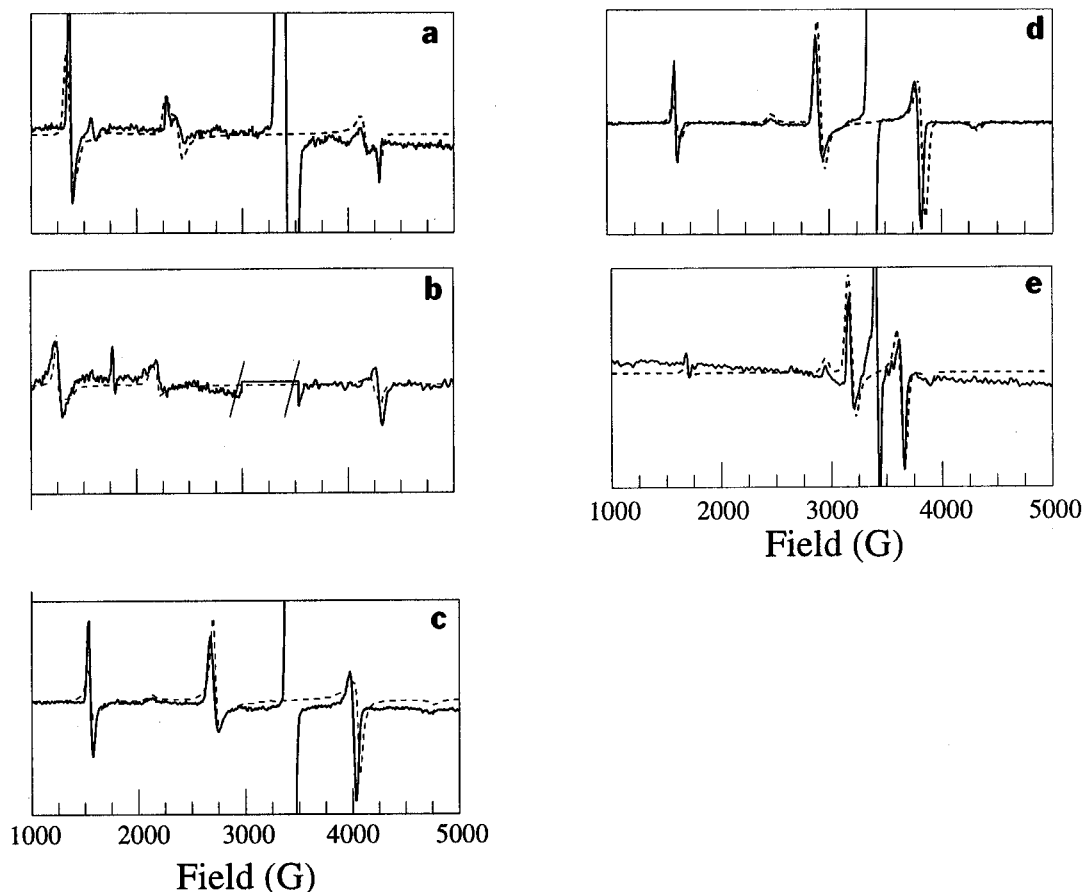(26) Ichimura, A. S. Unpublished results.

Figure 3. Biradical spectral regions (1000−5000 G) from photolysis of **6−10** at 77 K in MTHF (spectral traces a−e, respectively). All spectra were obtained at $\nu_0 = 9.5−9.6$ GHz. Dotted curves show spectral simulations using zfs parameters described in Table 1. All simulations used g_{iso} = 2.003 amd Gaussian line shapes with varying line widths.

Table 1. ESR Spectral Observations and Predictions for Species Derived from Photolysis of **6−10**

dinitrene	$\Delta E(S \rightarrow T)^a$	$|D/hc| \ (|E/hc|)^b$	$|D_{dipolar}/hc|^c$	$|D/hc|$ nitrene^d
1	574 (200)	0.169 (0.004)	0.0156	0.90
2	580(202)	0.188 (≤0.002)	0.0028	0.83
3	480(168)	0.122 (<0.002)	0.0015	0.74 (0.96)
4	677(237)	0.0865 (<0.002)	0.0009	0.66 (0.92)
5	145(51)	0.0442 (<0.001)	0.0004	0.63 (0.94)

^{a} Singlet−triplet energy gaps in cal/mol (cm^{-1}) from Figure 3 plots. ^{b}Experimental zero field splitting (zfs) parameters for dinitrenes in cm^{-1}. ^{c}Predicted zfs parameters for dinitrenes in cm^{-1} by the dipolar approximation of eq 2. ^{d} Experimental zfs parameters for mononitrene peaks associated with dinitrenes **1−5**, in cm^{-1}. Numbers in parentheses are assigned to less conjugated dinitrene geometries, as described in the text.

singlet ground state. Such difficulty in finding a qualitative match between theory and experiment has been observed in other weakly exchange coupled systems, notably tetramethyleneethane (TME).[27,28]

Biradicals **2** and **3** were reported in early UV−vis studies by Reiser and co-workers.[29,30] We later described some ESR spectroscopic studies of biradicals **2** and 3, and found them to have singlet biradical ground states with apparently quinonoidal nature.[3,4] Yabe and co-workers have studied **2** by UV−vis and IR spectroscopy, and used ESR spectroscopic evidence as a function of irradiation time to suggest the existence of a bisected

form of **2**.[31] The same group recently looked at the zfs and singlet−triplet gaps of **3** and the related 4,4′-azobenzene dinitrene by ESR.[32] Finally, based on recent work with planar-constrained versions of **2** and with unconstrained **3**, Harder *et al.*[21] suggested that a bisected form of **2** need not be invoked to explain the extra mononitrene peaks observed by Yabe, but that the new peak may be caused by products of dark reactions of planar **2** with the matrix solvent over 2 h or more. In addition, the studies of Harder *et al.* strengthened the argument that formation of the quinonoidal dinitrenes occurs via sequential deazetation reactions, rather than by double deazetation. The various studies of biradicals **2** and 3 and their corresponding mononitrenes have shown that not all the minutiae of these photoreactions are understood. Fortunately, our primary interest lies in comparison of trends among the zfs and ground state spin multiplicities of the biradicals **1−5** and related mononitrenes, which are readily obtained by ESR spectroscopy alone.

Table 1 shows that the zfs values of both the biradicals and the peaks in the corresponding mononitrene regions decrease monotonically along the series **2−5**. Biradical **1** has a smaller zfs than one might expect from this series. However, **1** is the only biradical of this set that does not have two phenyl rings, and therefore may be inappropriate for zfs comparison to **2−5**, save as being a member of the general family of these quinonoidal biradicals. The decease in mononitrene zfs as conjugation is extended in **6−10** is consistent with increasing delocalization of the mononitrene π-electron.

(27) Nachtigall, P.; Jordan, K. D. *J. Am. Chem. Soc.* **1992**, *114*, 4743.
(28) Nachtigall, P.; Jordan, K. D. *J. Am. Chem. Soc.* **1993**, *115*, 270.
(29) Reiser, A.; Wagner, H. M.; Marley, R.; Bowes, G. *Trans. Faraday Soc.* **1967**, *63*, 3162.
(30) Reiser, A.; Wagner, H. M.; Marley, R.; Bowes, G. *Trans. Faraday Soc.* **1967**, *63*, 2403.

(31) Ohana, T.; Kaise, M.; Yabe, A. *Chem. Lett.* **1992**, 1397. Ohana, T.; Kaise, M.; Nimura, S.; Kikuchi, O.; Yabe, A. *Chem. Lett.* **1993**, 765.
(32) Nimura, S.; Kikuchi, O.; Ohana, T.; Yabe, A.; Kaise, M. *Chem. Lett.* **1996**, 125. Cf. also the discussion of the comparative ESR spectra for 4,4′-stilbenedinitrene (**3**) and 4,4′-azobenzenedinitrene in ref 10.
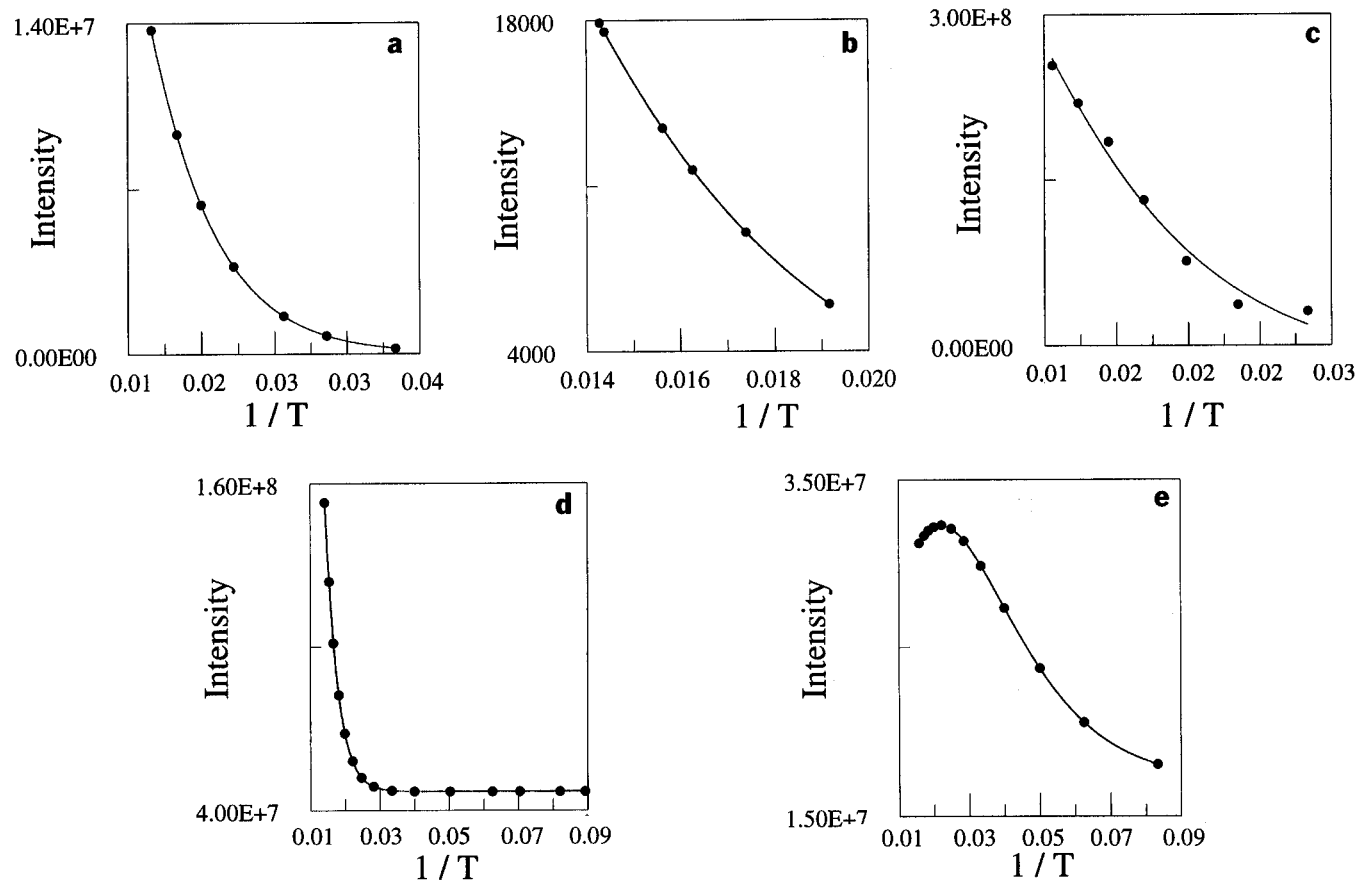
Figure 4. Curie law plots of ESR spectral intensity (I) versus reciprocal absolute temperature ($1/T$) for dinitrenes **1**−**5**. Fitted curves were obtained by nonlinear least-squares analysis based on eq 1; in some cases an ordinate offset parameter was used to allow for a non-zero intercept.

Conformations of Biradicals 1−5. The narrowness of the ESR spectral lines for **3**−**5** suggests that the triplet biradicals are not formed in a distribution of greatly different conformers. Further support for this notion was provided by photolysis of a sample of diazide precursor **10** that consisted of a mixture of geometric isomers, rather than being the *all-trans* material shown in Figure 1. When *all-trans* **10** is photolyzed, the fairly clean biradical spectrum of Figure 3e is observed. Figure 5 shows the ESR spectrum from photolysis of the geometrically mixed **10**. One can identify two sets of biradical peaks, one from the all-*trans* biradical with $|D/hc| = 0.0442$ cm^{-1}, and an inner spectrum with $|D/hc| \approx 0.018$ cm^{-1}, which we assign to a biradical with one or more *cis* or otherwise twisted ethylenic units. Using simulations (Figure 5, dotted curve) generated by summing various ratios of the two spectra, an approximately 1:5 mix of all-*trans* to highly twisted biradicals appears to be present in this sample. But, based on the simplicity of the biradical spectra when all-*trans* polyenes are used, we feel the evidence points to one major conformation for each triplet ESR spectral carrier, presumably an extended or nearly extended conformation.

The mononitrene regions of the spectra in Figures 2 and 5 also suggest that some complexity of geometry is possible. In addition to the mononitrenes whose zfs parameters are descrbed in Table 1 as corresponding to partial photolysis of diazides **6**−**10**, it is also possible to discern other peaks corresponding to mononitrenes with large zfs. Such a peak is not observed from diazide **6**, which has no possible conformational uncertainty. Biphenyl-based diazide **7** is known to show complex behavior of its mononitrene region, for reasons that have been assigned both to conformational torsion[31,32] and to low-temperature reactions[21] in the matrix. However, the variation in zfs of the mononitrene peaks derived from **7** is fairly small.

Photolysis of diazides **8**−**10** could in principle lead to conformational mixtures, if bond rotations or *cis-trans* isomerization were to occur in the matrix due to local heating effects. Table 1 shows in parentheses the zfs values of low-intensity mononitrene peaks which appear to be due to such effects. The high zfs in these species probably is due to production of deconjugating torsion during photolysis (or possibly due to photolysis of highly twisted conformers that are frozen in place by the low-temperature matrix). Torsional deconjugation reduces delocalization of the mononitrene π-electron, causing the higher zfs. A variety of geometric torsions is possible as the polyene chain length extends. Despite the presence of these "extra" dinitrene peaks, it appears that fairly specific geometries are required to produce the biradical spectra of **1**−**5**, based on the narrow lines in these spectra. This is consistent with the notion that torsion which decreases conjugation would both increase zfs in the mononitrenes derived from **8**−**10** and tend to truncate the exchange interactions which lead to the biradical states. This analysis, of course, evades the possibility of nitrenes derived from arylnitrene "ring-walk" rearrangement chemistry, which might well occur upon extensive photolysis.[33] In general, our assignment of the aryl mononitrene ESR peaks is perhaps best supported for putative structures with low zfs caused by increasing conjugation of the π-electrons, with the assignments for the low-intensity, higher zfs peaks being more tentative.

Ground State Spin Multiplicity. One may consider the expected ground state spin multiplicities of **1**−**5** from either a molecular orbital (MO) or valence bond (VB) point of view. In a MO model, Hund's multiplicity rules have frequently been

---

(33) Review of the rearrangement chemistry of arylnitrenes may be found, for example, in Wentrup, C. *Reactive Molecules. The Neutral Reactive Intermediates in Organic Chemistry*; Wiley: New York, 1984; pp 212−219 and references cited therein.
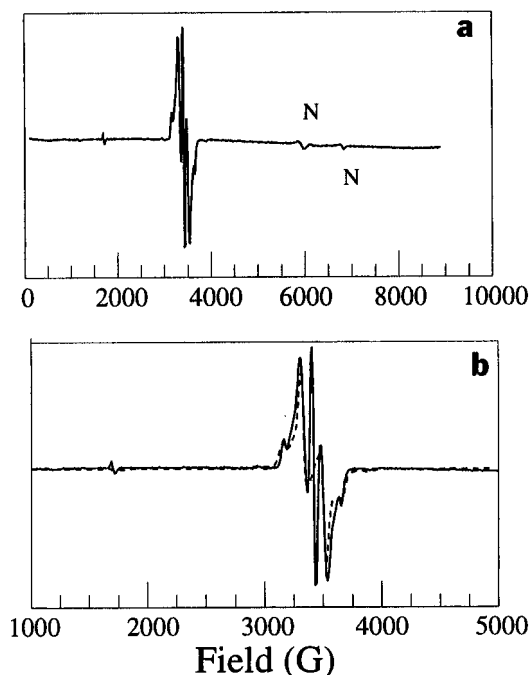
Figure 5. ESR spectrum at 9.58 GHz from photolysis at 77 K in frozen MTHF of a mixture of geometric isomers of diazide **10** (trace a, 0−10,-000 G). Trace b shows a 1000−5000 G blowup of curve a (solid line), compared to the simulation (dotted line) of a spectrum that is a 1:5 sum of triplet spectra with $|D/hc| = 0.0442$ cm^{-1} ($E = 0.000$ cm^{-1}) and $|D/hc| = 0.0180$ cm^{-1} ($E = 0.000$ cm^{-1}); both simulations use $g_{iso} = 2.003$ and Gaussian line shapes. The symbol "N" denotes a mononitrene peak.

applied to molecules having degenerate or near-degenerate biradical orbitals, with the result that a triplet ground state is predicted. However, in a variety of conjugated systems the Hund criterion is experimentally not followed, but rather a low-spin singlet state is found.[34] TME and its derivatives are simple hydrocarbon examples of such systems in the disjoint class of connectivity.[35]

The low-spin natures of TME and related disjoint systems have been interpreted as supporting VB-type models of electronic exchange. Various derivations have been given by Ovchinikov,[36,37] Klein,[38−40] Borden and Davidson,[35,41] and Sinanoglu,[42] *inter alia*, in order to model intramolecular exchange in connectivity-conjugated systems that are not properly treated by the simplistic MO plus Hund's rule model. A more general theme involves use of spin polarization (SP) arguments to understand the distribution of spin densities in an open-shell system.

SP arguments are particularly useful for interpreting the behavior of localized biradicals **1−5**, since these are not readily treated by the connectivity-based models described above. Most

(34) Borden, W. T.; Iwamura, H.; Berson, J. A. *Acc. Chem. Res.* **1994**, *27*, 109.

(35) Borden, W. T.; Davidson, E. R. *J. Am. Chem. Soc.* **1977**, *99*, 4587.

(36) Misurkin, I. A.; Ovchinnikov, A. A. *Russ. Chem. Res. (Engl).* **1977**, *46*, 967.

(37) Ovchinnikov, A. A. *Theor. Chim. Acta* **1978**, *47*, 297.

(38) Klein, D. J.; Nelin, C. J.; Alexander, S.; Matsen, F. E. *J. Chem. Phys.* **1982**, *77*, 3101.

(39) Klein, D. J. *Pure Appl. Chem.* **1983**, *55*, 299.

(40) Klein, D. J.; Alexander, S. A. In *Graph Theory and Topology in Chemistry*; King, R. B., Rouvray, D. H., Eds.; Elsevier: Amsterdam, The Netherlands, 1987; Vol. 51, pp 404.

(41) *Diradicals*; Borden, W. T., Ed.; John Wiley and Sons, Inc.: New York, 1982.

(42) Shen, M.; Sinanoglu, O. In *Graph Theory and Topology in Chemistry*; King, R. B., Rouvay, D. H., Eds.; Elsevier: Amsterdam, The Netherlands, 1987; Vol. 51, pp 373−403.
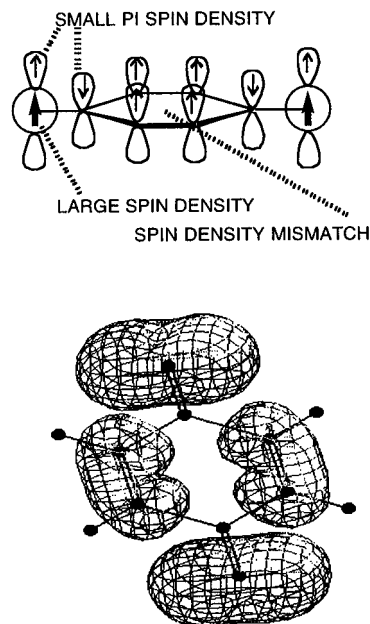
Figure 6. Spin polarization diagram for dinitrene **1**, and a spin−spin density map for **1** (6-31G* UHF-SCF level, standard SPARTAN settings). In the spin polarization diagram, the bottom π-orbital lobes of distant carbons were omitted for clarity in presentation.

of the spin density in the triplet states of **1−5** is localized in two singly-occupied σ orbitals (SOMOs) on the terminal nitrogen atoms. These large spin populations polarize the π-electrons that are nearby, particularly the nitrogen π-electrons. *It is important to remember that the total π spin density sums to zero over all sites, but that individual sites may be polarized to have positive or negative non-zero densities.* Each nitrogen SOMO has a large α spin density, which by SP causes a small, positive α spin density in the nitrogen π-space. Throughout the rest of the π-orbital subspace, one expects the usual SP rules to apply, such that each orbital of α spin density prefers to be attached to sites with β spin density, and vice versa. This is illustrated for biradical **1** in Figure 6. The same figure also shows a spin density map of the $^3B_{1u}$ state of **1**, using a 6-31G* UHF wave function and the SPARTAN graphical interface.

For triplet states of **1−5** a spin mismatch occurs in the π-space (Figure 6), with destructive interference occurring between adjacent sites having the same sign of spin density, destabilizing the triplet relative to the singlet state. Thus, the singlet should be the ground state by a small amount, as is experimentally observed. Any effects of heteroatom substitution appear insufficient to reverse SP effects favoring a singlet state. In a similar manner, the connectivity analogous dicarbenes **11−12**[43] are found to be low-spin ground states with low-lying triplet biradical states. The spin density distribution in **12** is found by ENDOR to be qualitatively just as shown in Figure 6, further supporting the SP model for **1−5**.

A Model for Zero Field Splitting Magnitudes in 1-5. The same SP model used to explain the qualitative ground state multiplicities for **1−5** can explain the semiquantitative trends in zero field splitting (zfs). In the most simplistic picture of these biradicals, the triplet state has two electrons localized into different σ SOMOs on the terminal nitrogens. A simple dipole−dipole approximation to the zfs may be made using eq 2,[44] where

(43) Teki, Y.; Sato, K.; Okamoto, M.; Yamashita, A.; Yamaguchi, Y.; Takui, T.; Kinoshita, T.; Itoh, K. *Bull. Magn. Reson.* **1992**, *14*, 24.

(44) A variant of eq 2 with different units is found in: Eaton, S. S.; More, K. M.; Sawant, B. M.; Eaton, G. R. *J. Am. Chem. Soc.* **1983**, *105*, 6560.

g is the free electron g value and r_{ij} is the distance in angstroms between interacting dipoles.

$$D \ (\text{cm}^{-1}) = 1.299g/r_{ij}^{3} \tag{2}$$

This equation shows that zfs should decrease rapidly as r_{ij} increases. Table 1 compares experimental zfs for **1**−**5** to zfs predicted using eq 2, where r_{ij} is taken as the distance between the nitrogen atoms in a triplet UHF AM1 optimized geometry for each biradical. Use of slightly more sophisticated models—such as splitting the unpaired spin population on each nitrogen into the two halves of a localized Slater type p-orbital—does not change these numbers appreciably. As the distance between nitrogen atoms increases in **1**−**5**, the predicted zfs rapidly decreases to a negligible amount. This is not what is experimentally observed. Conformational effects cannot be invoked to explain the whole discrepancy, since planar **1**−**3** already have zfs far larger than expected by the dipole−dipole model. In addition, none of **1**−**3** have sufficient conformational flexibility to allow the terminal nitrogens to come close enough to explain the observed zfs by a through space effect.

But, if unpaired spin density is distributed throughout the molecules by the SP model, there are interactions between the large, localized spin population in the nitrogen σ space and the small, polarized spin sites that are distributed throughout the conjugated π-space. All of the π-spin populations are quite small, but due to the r_{ij}^{3} dependence of the dipolar interaction, the one-center terms involving the large localized σ spin density and the small π-spin density on each nitrogen dominate. This one-center interaction looks similar to the interaction which makes the zfs in a mononitrene so large,[45] but is different because the nitrogen π-spin population in **1**−**5** is very small. In fact, the α π-spin density on each nitrogen in the biradicals is explicable only when spin polarization effects are considered, and hence is not a simple zeroth-order effect. As the length grows of the π-conjugated network separating the localized nitrogen electrons, the polarized π-spin density on each nitrogen grows smaller through delocalization, while the localized spin density remains about the same. As a result, the zfs should decrease throughout the series **2**−**5**, as observed.

An early model of the zfs for **1** was given by Serre and Schneider,[46] using a simple MO approximation to the spin density distribution that is qualitatively similar to the depiction of Figure 5. Details of the calculation were not given, but the predicted result of (−)0.181 cm^{-1} compared favorably to the known zfs of 0.17 cm^{-1}. In an effort to make a similar estimate, we used the Lowdin spin density distribution at a 6-31G* SCF-MO-SDTQ-CI level of theory.[25] We then computed the sum of purely dipolar zfs contributions between all pairs of spin density sites ρ_i and ρ_j, as shown in eq 3. We simulated each

$$D \ (\text{cm}^{-1}) = 1.299g\left(\sum_{i>j}\rho_i\rho_j/r_{ij}^{3}\right) \tag{3}$$

π-type spin density site as a point spin split equally onto the two lobes of a p-orbital, with each half-density placed at a distance from the associated atom equal to the radius of the equivalent Slater type orbital. This method follows the approach used by Berson and co-workers for zfs predictions, details of which are given elsewhere.[47] This is an approximate methodol-

ogy, but should suffice for order of magnitude estimates to determine the major contributions to the overall zfs of **1**. Details of the geometry and spin population numbers used in the calculation are given in the Supporting Information. While variation in the exact spin populations used in this calculation will effect the value estimated for **1**, we shall see below that the simple extension of the dipolar model to include one-center interactions, as done in the earlier work of Serre and Schneider, makes a critical difference in the order of magnitude estimate of the zfs.

Table 1 gives the zfs expected from eq 3 when π-spin polarization is ignored, and all spin density is assumed to be in the localized orbitals. All such estimated zfs are found to be far too small to fit the experimental facts. But, when the 6-31G* SCF-MO-SDTQ-CI spin density distribution is used for **1**—thus incorporating one-center interactions—the estimated zfs for **1** is ∼0.2 cm^{-1}, reasonably close to the observed value of 0.169 cm^{-1}. The one-center s−p interactions on the nitrogen sites contribute most of the zfs in the estimate based upon eq 3. As a result, we feel that the SP model for the triplet state of **1** is both appropriate and sufficient to explain its large zfs.[48]

At present, we have not extended this semiquantitative model to the larger systems **2**−**5**, due to the difficulty involved in ab initio spin density computations for the larger systems. Single-determinant UHF calculations tend to be badly spin contaminated, even with 6-31G* and higher basis sets. In addition, without reasonably good geometries, we feel that spin density distribution estimates for **2**−**5** will not be quantitatively useful. Multiconfigurational CASSCF calculations appear to be promising for spin density distributions in these molecules but are computationally very demanding. At present, we are still working on a practical theoretical approach to this problem. Still, the qualitative SP-based arguments appear to be consistent with experimental facts observed for zfs trends in **2**−**5**.

Summary. The singlet state biradicals **1**−**5** are the products of fascinatingly complex photochemistry. Although this class of biradicals have been known for about 30 years, it has remained for recent work to show clearly that the triplet ESR spectra observed for these molecules are due to excited states, and that the unusually large zfs observed for the triplets is commensurate with the spin polarization models that are have become most useful to describe open shell molecules. Although these molecules are not obvious candidates for practical use in the development of new organic-based magnetic materials, they are of considerable use in allowing the investigation of the exchange interaction between unpaired electrons, a key facet in molecular magnetism. We anticipate that these biradicals will be of further interest in solid state matrix investigations[9] that are continuing at present.

Experimental Section

General. All chemicals were obtained from Aldrich Chemical Co. unless otherwise noted. 2-Methyltetrahydrofuran was distilled from lithium aluminum hydride and tetrahydrofuran from potassium/benzophenone, both under argon.

Ultraviolet−visible spectra were obtained on a Shimadzu UV-260 double-beam spectrometer, and tetrahydrofuran was used as a solvent in all measurements. Infrared spectra were obtained on a Perkin-Elmer 1420 spectrophotometer, and were referenced against polystyrene at 1601 cm^{-1}. ^{1}H-NMR spectra were obtained on an IBM Instruments NR-80A Fourier transform spectrometer, and were referenced against

(45) Wasserman, E. *Prog. Phys. Org. Chem.* **1971**, *8*, 319.

(46) Serre, J.; Schneider, F. *J. Phys. Chim.* **1964**, *61*, 1655.

(47) Rule, M.; Matlin, A. R.; Seeger, D. E.; Hilinshi, E. F.; Dougherty, D. A.; Berson, J. A. *Tetrahedron* **1982**, *38*, 787. Cf. also: Hilinski, E. F. Ph.D. Thesis, Yale University, New Haven, CT, 1982. The latter reference contains a listing of the program used for zfs prediction by the methods listed this paper.

(48) It is also plausible that spin−orbit coupling contributes to the overall zfs of **1**−**5**. However, the spin−orbit coupling constant of atomic nitrogen is small, only 76 cm^{-1} (Gordy, W. In *Techniques of Chemistry*; West, W., Ed.; Wiley, New York, 1980; Vol. XV, p 604). While a spin−orbit contribution is thus possible, the analysis in the main text suggests that this contribution is not required to explain the size of the zfs.

internal tetramethylsilane on the delta (δ) scale in parts per million. Chemical analyses were performed by the University of Massachusetts Microanalysis Laboratory.

Electron spin resonance (ESR) spectra were obtained on a Bruker ESP-300 X-band spectrometer attached to a standard Bruker data system allowing multiscan spectral digitization and analysis. ESR peak positions are reported in units of gauss referenced against neat diphenylpicrylhydrazyl ($g = 2.0037$), and peak intensities were obtained by computer-aided double integration using standard Bruker software routines. Further details of ESR spectral acquisition are described in the section on Nitrene Generation. All ESR spectral simulations were carried out on a Silicon Graphics R4000 computer using a program that uses the eigenfield method described elsewhere.[18]

1,4-Diazidobenzene. In a 200-mL round-bottom flask was placed a solution of 1.0 g (15 mmol) of sodium azide in 77 mL of distilled water. The flask was placed in an ice bath, treated with 1.9 g (6.3 mmol) of 1,4-phenylenebis(diazonium tetrafluoroborate) (see Supporting Information), and stirred for 30 min. The resultant precipitate was collected by filtration, washed with water, then dissolved in ethyl ether. The ether solution was dried over magnesium sulfate and treated with decolorizing charcoal. The solvent was evaporated to give 0.7 g (70%) of light yellow/orange powder with mp 80−81 °C (lit.[30] mp 80 °C) Anal. Calcd: C, 45.0, H, 2.5; N, 52.5. Found: C, 44.50; H, 2.66; N, 51.90%. ^{1}H-NMR (80 MHz, CDCl$_3$): δ 7.6 (s, Ar-H). IR (KBr; cm^{-1}): 2080 and 2110 (s, −N$_3$ str). UV−vis (λ_{max} [ϵ]; nm [M^{-1} cm^{-1}]): 272 [12 400].

4,4′-Diazidobiphenyl (7). This compound was synthesized as described previously by us.[3] The product was a buff-colored solid with mp 120−122 °C (lit.[30] mp 127−128 °C). Anal. Calcd: C, 61.0; H, 3.4; N, 35.6. Found: C, 61.06; H, 3.78; N, 33.4. ^{1}H-NMR (CDCl$_3$, 80 MHz): δ 6.8−7.2 (para AA′BB′ q, 4 H, $J = 8.0$ Hz, Ar-H). IR (KBr; cm^{-1}): 2130 (s, −N$_3$ str). UV−vis (λ_{max} [ϵ]; nm [M^{-1} cm^{-1}]): 297 [36 700].

(E)-4,4′-Diazidostilbene (8). In a 30-mL round-bottom flask were placed a solution of 2.1 mL of concentrated hydrochloric acid in 3.8 mL of distilled water, followed by the addition of 1.0 g (4.8 mmol) of (E)-4,4′-diaminostilbene (Supporting Information). The flask was placed in an ice bath. The mixture was treated dropwise with a solution of 0.69 g (10 mmol) of sodium nitrite in 2.4 mL of distilled water. The mixture was stirred for an additional 1 h in the ice bath, then filtered to remove any undissolved impurities. The solution was placed in the ice bath and treated with a solution of 0.62 g (9.5 mmol) of sodium azide in 2.4 mL of distilled water. Gas evolution was observed immediately after the addition of sodium azide solution. The mixture was stirred in the ice bath for 15 min. The resultant precipitate was collected by filtration, dried under vacuum, dissolved in chloroform, treated with decolorizing charcoal, and dried over magnesium sulfate. The solvent was evaporated and the resultant solid was dried under vacuum. The product was 0.71 g (57%) of light brown solid with mp 154−155 °C (lit.[30] mp 164 °C). Anal. Calcd: C, 64.1; H, 3.8; N, 32.9. Found: C, 63.19; H, 3.73%; N, 31.42. ^{1}H-NMR (CDCl$_3$, 80 MHz; ppm): δ 7.0 (s, 4 H, −CH=), 6.95−7.75 (para AA′BB′ q, 8 H, $J = 8.8$ Hz, Ar-H). IR (KBr; cm^{-1}): 2130 (s, −N$_3$ str), 960 and 975 (s, *trans* −CH=CH− oop bend). UV−vis (λ_{max} [ϵ]; nm[M^{-1} cm^{-1}]): 341 [34 400].

(E,E)-Bis(p-azidophenyl)-1,3-butadiene (9). In a 25-mL round-bottom flask were placed 0.3 g (1.3 mmol) of (E,E)-bis(p-aminophenyl)-1,3-butadiene (Supporting Information) and 1.6 mL of a 5.6/10 (v/v) solution of dilute hydrochloric acid in water. The flask was placed into an ice bath. The mixture was then treated with a solution of 0.18 g (2.6 mmol) of sodium nitrite in 0.6 mL of distilled water over 30−40 min, the solution foamed during the addition of sodium nitrite solution. The mixture was further stirred for 1 h in the ice bath. The mixture was treated dropwise with a solution of 0.17 g (2.6 mmol) of sodium azide in 0.6 mL of distilled water; the mixture foamed during the addition of sodium azide solution. The mixture was next diluted with distilled water and stirred for 20 min. The resultant precipitate was collected by filtration and dried under vacuum, redissolved in methylene chloride, treated with decolorizing charcoal, and dried over magnesium sulfate. The solvent was evaporated, and the residue was passed through a silica gel column with methylene chloride as the eluent. The solvent evaporation gave 0.07 g (18%) of orange solid which decomposed and turned black upon heating at 120−130 °C. Samples of the solid darkened within 3 min of exposure to fluorescent lighting. Anal. Calcd: C, 66.7; H, 4.2; N, 29.1. Found: C, 66.43; H, 4.01; N, 28.83. ^{1}H-NMR (CDCl$_3$, 80 MHz; ppm): δ 6.6−7.0 (m, 4 H, −CH=), 7.0−7.4 (*para* AA′BB′ q, 8H, $J = 8.7$ Hz, Ar-H). UV−vis (λ_{max} [ϵ]; nm [M^{-1} cm^{-1}]): 361 [47 500], 301 [33 700], 348 [39 100]. IR (KBr; cm^{-1}): 2130 (s, −N$_3$ str), 990 (s, *trans* −CH=CH− oop bend).

1,8-Bis(p-azidophenyl)-1,3,5,7-octatetraene (10). Method A: In a 100-mL round-bottom flask were placed 37 mL of distilled water, 2.7 mL of concentrated sulfuric acid, and 2.25 g (7.80 mmol) of 1,8-bis(p-aminophenyl)-1,3,5,7-octatetraene (Supporting Information). The mixture was heated to 60 °C by an oil bath and stirred for 2 h, then quickly cooled with an ice bath and treated with dropwise addition of a solution of 1.19 g (17.2 mmol) of sodium nitrite in 3.7 mL of distilled water over 40 min. The mixture was stirred for an additional 20 min in the ice bath and then diluted with 148 mL of cold distilled water and treated with a solution of 1.01 g (15.5 mmol) of sodium azide in 5.0 mL of distilled water. The mixture foamed and a precipitate appeared, as the reaction color changed from deep purple to colorless. The precipitate was collected by filtration in subdued light and dried under vacuum to give 0.5 g (19%) of ruddy solid product. Samples of the solid turned dark within 3 min of exposure to fluorescent lighting. Upon heating, the compound blackened without liquefaction at temperatures above 180 °C. ^{1}H-NMR (DMSO-d_6, 80 MHz): δ 6.4−6.9 (br m, 8 H, −CH=), 6.9−7.4 (*para* AA′BB′ q, 8 H, $J = 8$ Hz, Ar-H). IR (KBr; cm^{-1}): 2110 (s, −N$_3$ str).

Method B: All glassware was flame dried before use. In a 250-mL three-necked round-bottom flask were placed 140 mL of absolute ethanol, 4.5 g (7.0 mmol) of 4-azidobenzaldehyde (Supporting Information), and 2.6 g (18 mmol) of hexa-2,4-diene-1,6-diylbis(tributylphosphonium) dibromide (Supporting Information). The flask was purged with nitrogen. A sodium ethoxide solution was prepared by dissolving 0.48 g (21 mmol) of sodium metal in 21 mL of absolute ethanol. The flask was placed in an ice bath, then treated dropwise with a sodium ethoxide solution while stirring. The flask was warmed to room temperature and stirred under nitrogen overnight. This compound is a mixture of geometric isomers which may be isomerized by boiling in acetone with a crystal of iodine for up to 10 h under inert atmosphere in the dark. The final product gives the same spectoscopic data as the product produced by method A. Upon heating, the compound did not melt, but blackened without liquefaction at temperatures above 180 °C. No further purification was done due to the photolytical instability of the product.

Diazide Photolysis and Variable Temperature Analyses. Azides were irradiated for 5 min using a 1000-W Xenon arc lamp with Pyrex filter at 77 K. The samples were prepared by dissolving the appropriate azide compound in dry 2-methyltetrahydrofuran, approximate concentration of 1 mg/1 mL. The sample was placed in a Wilmad 707SQ Suprasil 4 mm o. d. quartz ESR tube, subjected to three freeze−pump−thaw vacuum degassing cycles, and sealed under vacuum. Next, the sample was frozen at 77 K in a Wilmad liquid nitrogen finger dewar (WG-816-B-Q Suprasil), subjected to photolysis, and directly placed into a precooled ESR cavity. For fixed 77 K experiments, the cavity cooling was provided by a second finger dewar charged with liquid nitrogen. For lower temperature work, an Oxford Instruments ESR-900 liquid helium cryostat precooled to 50 K was used, and the sample transferred from the finger dewar into the crystat with sufficient swiftness that sample thawing did not occur. Typically, upon thawing the irradiated sample solutions turned deep red within 60 s, then faded within another 60 s to a straw colored solution containing a red solid.

For all Curie plots, intensities were judged by double integration of a reasonably strong, free-standing peak in each spectrum. Integration limits were kept constant for any spectrum as the temperature was varied. Intensity measurements were obtained both with decreasing and increasing temperature, to assure that there were no appreciable effects of sample decomposition or annealing over the temperature ranges used. Temperatures were measured in the Oxford ESR-900 cryostat by an AuFe/chromel thermocouple placed just below the sample position; the temperatures were calibrated against carbon electrodes. Saturation effects were avoided by running all spectra at microwave powers of ≤ 1 mW (100 kHz modulation amplitude).

Supporting Information Available: Synthetic and analytical data for a number of intermediates in the syntheses of diazides **8**−**10** and for 4-azidobenzaldehyde, a tabular summary of peak positions for the ESR spectra in Figure 2, and details of data used in the zfs estimate for **1** (8 pages). See any current masthead page for ordering and Internet access instructions.

JA963648D